PRJ, Vol. 6 (January 1994); P. 18–31, 29 FIGS, 3 TABLES.

FAILURE INVESTIGATION OF WELD JOINT BETWEEN MANURITE 36X AND INCOLOY 800H TUBES IN ETHYLENE PLANT CRACKING FURNACE

M.L. Mahta* and A.T. Hassan**

دراسة حالة الإخفاق بماسورة الوصل الملحومة بين أنابيب المارونايت 36X وأنكولوي 800H بفرن التكسير بمصنع الاثيلين

م. مهتا و عبد الفتاح حسن

تم القيام بأعمال الدراسة المجهرية وقياس التأثر بالمغناطيسية وتعيين كمية الكربون في مناطق مختلفة من منطقة اللحام، كما تم قياس الصلابة، وتعيين التركيب الكيميائي والتحليل بجهاز EDAX.

لقد تم تشقق اللحام في كامل سمك المادة مع وجود مواقع تكربن وتكون كربيدات في حدود الحبيبات وتولد طور رمادي. كما لوحظ وجود صلادة (عالية) بمواقع التكربن وتجاويف زحف/شقوق. التحليل بجهاز EDAX وضح أن الطور الرمادي المتكون عند حدود الحبيبات غنيا بمعدني المنجنيز والكروم.

بدا تشقق اللحام من الجذر نتيجة تكربن جذر اللحام وتولد الطور الرمادي سهل التقصف بحدود الحبيبات. وزاد تغلغل الشقوق بمساعدة الزحف المتزايد الناجم عن تركز الإجهادات بأطراف الشق والإجهاد العالي الذي تولد عن صغر مساحة اللحام التي تعرضت للضغط مع تطور الشق وتكون الطور الرمادي سهل التقصف بحدود الحبيبات.

ABSTRACT

Macroscopic study, magnetic susceptibility measurement, bulk carbon analysis of different regions of the weld, hardness masurement, chemical composition and Energy Dispersive of X-Ray Analysis (EDAX) were carried out. Localized carburization in the weld regions, formation of grain boundary carbides and grey phase, hardness at carburized locations and creep cavities/cracks were observed. EDAX revealed brittle grey phase formed at grain boundaries rich in Mn and Cr.

Initiation of weld cracking was from its root. This was caused by carburization of the root of the weld and the formation of brittle grey phase at grain boundaries through their embrittling effects. Propagation of cracks was assisted by enhanced creep due to stress concentration centration at crack tips and higher stresses caused by decreasing load bearing area of the weld with the progress of the fracture and formation of brittle grey phase at grain boundaries.

* Formerly with Petroleum Research Centre, Tripoli, Libya, G.S.P.L.A.J.

** Petroleum Research Centre, P.O. Box 6431, Tripoli, Libya, G.S.P.L.A.J.

INTRODUCTION

Ethylene is produced by cracking naphtha in the radiant coil tubes heated in the furnace. Cracking is accomplished at low pressures and elevated temperatures in the range 950–1100°C.

The environment within the radiant coil tubing is carburizing while that on the outside or fire box side is oxidizing.

The outlet of the tube is exposed to higher temperature coil tubes and decoked at regular intervals.

CASE HISTORY

Cracking occured in the outlet of the radiant tube of the coil and is marked in the Fig. 1. Crack was observed at weld joint between dissimilar tubes,

Manurite 36X and Incoloy 800H during operation of the furnace. The following is the pertinent data of the case:

Outlet pipe material: Manurite 36X-Incoloy 800H pipe.
Skin temperature during services: 1003–1035°C
Design temperature: 1080°C
Maximum operating pressure: 1.83 kg/cm^2
Design pressure: 5.4 kg/cm^2
Decoking carried out: 9 times during the furnace working time of 548 days.

higher susceptibility was observed from the root side.

Incoloy 800H was also found to be susceptible from the internal surface, while Manurite 36X was not susceptible in any region. Reason for localized development of magnetic susceptibility is localized carburization of the weld during service. Chromium is withdrawn from the matrix. This chromium depletion yields a matrix which becomes progressively more magnetic.

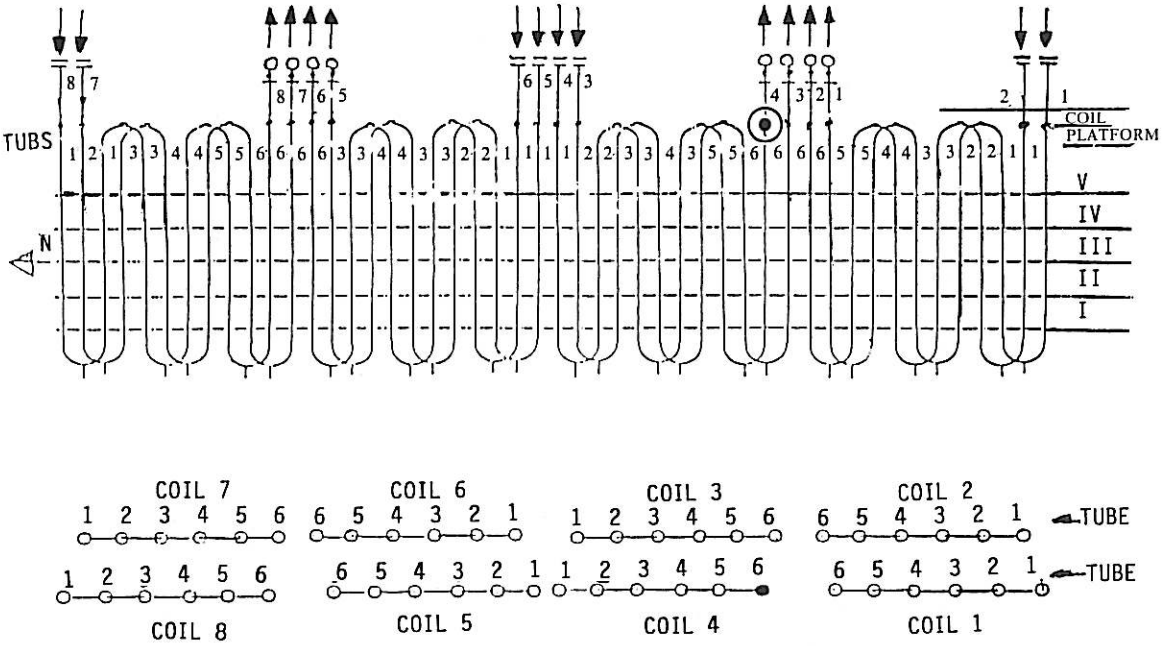


FIG. 1. Sketch of the radiant coil of cracking furnace 1-F-10-G with the location of crack (encircled).

INVESTIGATION

A. Magnetic Susceptibility

Metallographic observations revealed extensive formation of second phase precipitates in the area along the fracture surface of the weld. The magnetic susceptibility of the weld joint was to bring one of the poles close to the weld joint to detect susceptible and non-susceptible regions of the weld. For this measurement small samples containing the weld had to be cut for detecting magnetic susceptibility. Observations are marked in Fig. 2.

Regions of the weld cracked through thickness showed magnetic susceptibility while uncracked as well as partially crack regions were not found to be susceptible. For the susceptible region, weld away from the fracture was not susceptible indicating localized carburization. Further a

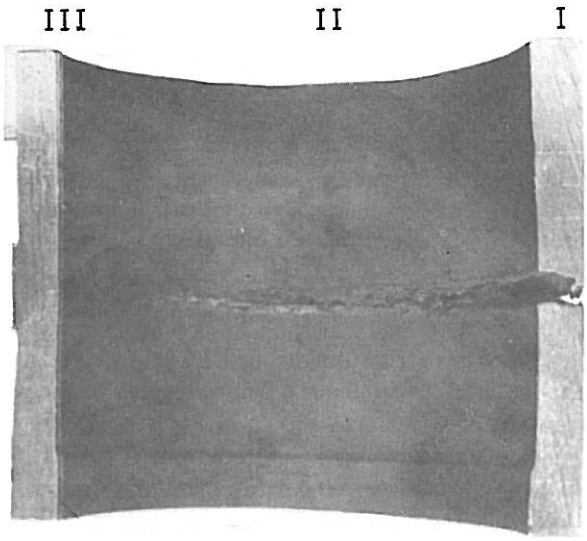


FIG. 2. Magnetically susceptible (MS) region of the weld (cracking through thickness) and nonsusceptible (NS) weld region marked on one of the equal halves of the tube.

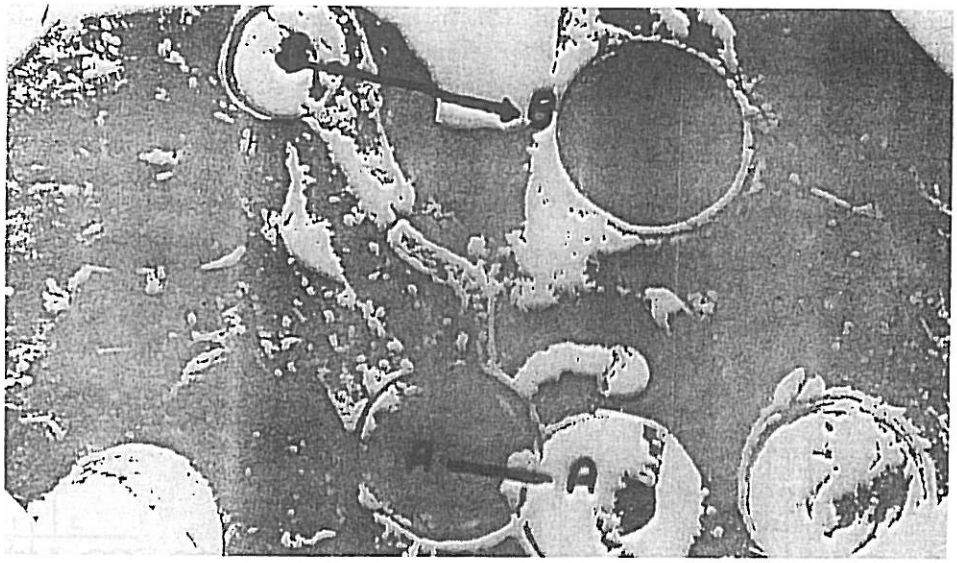


FIG. 3a. Three locations analysed for carbon analysis from the weld region partially cracked through thickness (i) A-A in the root region (ii) B-B around weld center line (WCL) near weld surface (OWS) (iii) C-C OWS but away from WCL.

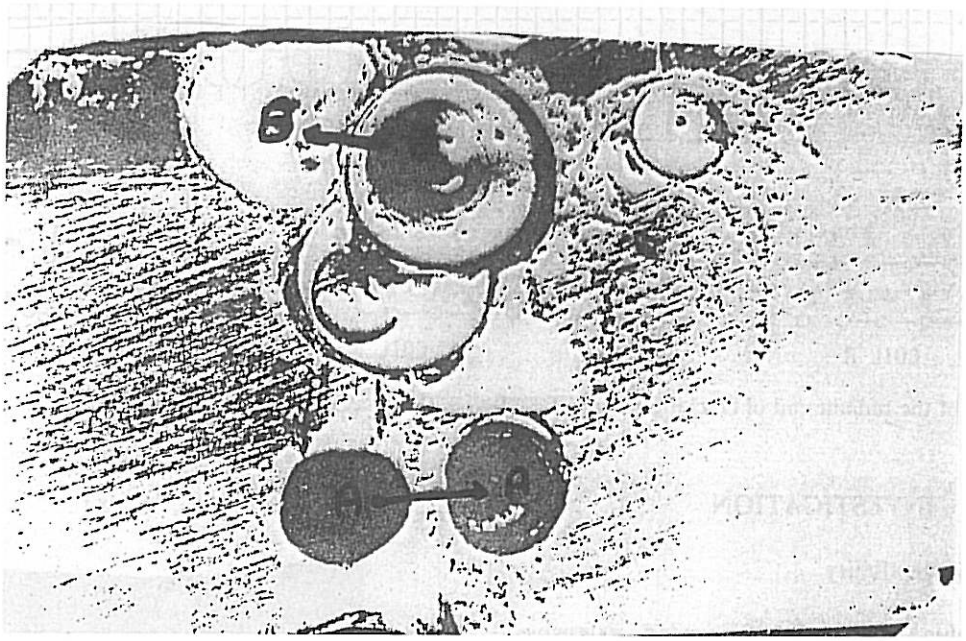


FIG. 3b. Two locations analysed for carbon analysis from the weld region free from cracks (i) A-A in the root region (ii) B-B around WCL near outer weld surface.

B. Carbon Analysis

This was carried out using LECO instrument on the material drilled from different regions of the weld (samples II and III) as shown in Figs. 3a, 3b.

Results are listed in Table 1. Sample II clearly indicates carburization in the root region and weld center line, while the weld near the outside surface but away from the center line, did not suffer from carburization.

Carbon contents in the carburized regions were 0.62 and 0.54 wt.% respectively, while it was 0.12 wt.% for the uncarburized regions. Sample II was magnetically susceptible from the fracture end as well as from the root side.

For sample III, free from cracking, carbon content in the outer weld region and that in the root region are different as seen in Table 1. However, the difference is not large enough to indicate carburization. This sample did not show magnetic susceptibility.

The inner surface Incoloy 800H tube suffered from carburization while the outer surface was not affected as evident from the results listed in Table 1.

Table 1. Bulk Carbon Analysis of Different Regions of the Weld

Location of samples	Weight of the sample (g)	Carbon content (wt.%)
1. As seen in Fig. 3a		
a. Root region of the weld designated as A-A	0.1957	0.620
b. Near outer weld surface in and around weld center line (WCL) region B-B	0.1454	0.540
c. Outer weld surface but away from the fracture surface region C-C	0.1612	0.120
2. As seen in Fig. 3b		
a. In the root pass region AA-	0.1636	0.155
b. Near outer weld surface region B-B	0.1559	0.102
3.		
a. Inner surface of Incoloy 800H tube	0.1426	0.441
b. Outer surface of Incoloy 800H tube	0.2839	0.129

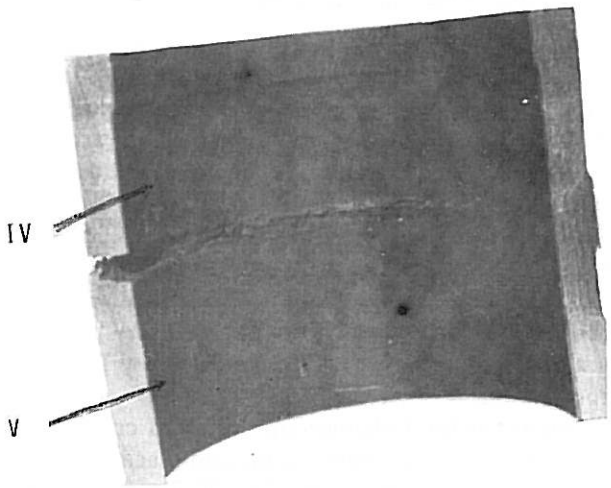


FIG. 4. Cross sections of the weld regions, from locations IV. V as indicated in the micrograph.

C. Hardness

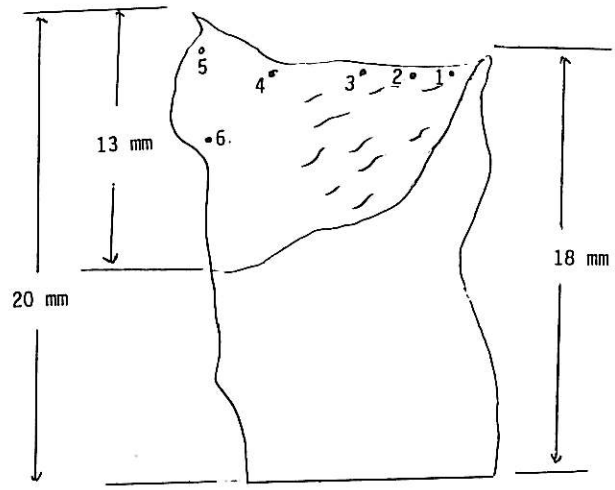
Hardness was measured in the cross-sections of the weld regions from locations IV, V indicated in Fig. 4 using Vickers Hardness Tester.

Locations, where hardness was measured, are shown schematically in Figs. 5a, 5b and 5c. Large hardness increase was detected along the fracture edge through the thickness of fracture region of the weld (Fig. 5a), near the outer weld surface. Away from the fracture edge the hardness was much lower, 158 HV5 as compared to 260 HV5 in the root, while in the region with multiple minute visible cracks in the root area (Fig. 5b) hardness recorded was higher than in the weld region free from cracks as evident from the results listed in Fig. 5b. In the weld region, which in the cross-section (Fig. 5c) showed a minute visible crack in the root region, hardness variation was not observed.

D. Metallographic Study

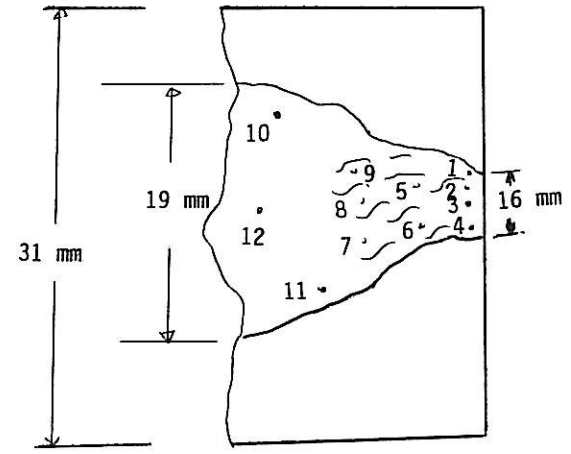
Samples I–III were taken from weld region and their location is depicted in Fig. 4. They were taken from weld region which had visible minute cracks/ crack in the root of the weld.

Sample I. Figure 6a is the microstructure of cross section fracture along the weld center line. Microstructures in the root region and those adjacent and away from the fracture in the weld are shown in Figs. 6b, 6c, 6d and 6e. Extensive precipitation in the root region and fracture region Fig. 6(b–d) were seen within grains. Precipitates, within the matrix, are attributed to the carbides resulting from carburization. Away from the fractured surface, precipitation is less extensive and is finer. Fig. 6e shows the formation of creep microcavities/voids along grain boundaries and the much finer precipitates. This region has not undergone carburization but suffered extensive creep damage. Grey phase at grain boundaries was detected in the root of the weld as well as in the filler passes as in Figs. 6b and 6f. This phase is porous and brittle.



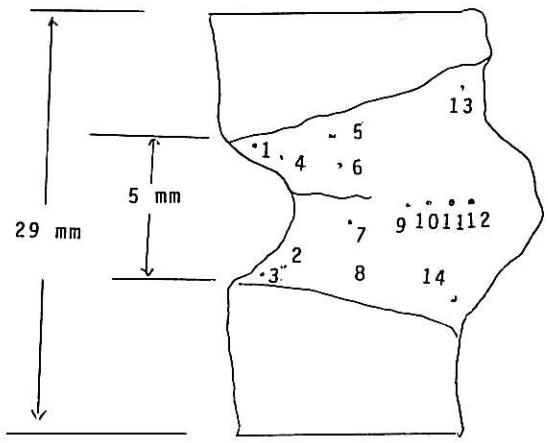
Location of hardness measurement	Hardness HV5
1	260
2	262
3	268
4	246
5	166
6	158

FIG. 5a. Schematic representation of locations of hardness measurements and hardness values in weld region shown in Fig. 6a revealing high hardness in the fracture end.



Location of hardness measurement	Hardness HV5
01	229
02	186
03	172
04	161
05	178
06	172
07	157
08	172
09	162
10	161
11	157
12	157

FIG. 5b. Schematic representation of locations of hardness measurement and hardness values in weld region shown in Fig. 8a revealing higher hardness in the root of the weld.



Location of hardness measurement	Hardness value HV5
01	153
02	158
03	157
04	153
05	153
06	152
07	156
08	157
09	160
10	156
11	156
12	162
13	153
14	157

FIG. 5c. Schematic representation of location of hardness and hardness values in weld region shown in Fig. 9a.

Sample II. Figure 7a give the macrostructure of section of the weld region showing cracking in the root region of the weld and cracks, away from the weld center line. Figures 7c and 7d show cracks in the root and extensive precipitates of different shapes.

Grain boundaries precipitates and some of precipitates in the matrix are attributed to carbides. These microstructural changes indicate carburization of the root region of the weld. Formation of grey phase at grain boundaries was also observed away from the root region.

Microstructural changes are less, and creep damage in the form of cavities/voids and cracks are seen as illustrated in Fig. 7e and Fig. 7f. Precipitates are much finer and such microstructural changes are observed in the later part of the third stage creep.

Sample III. Macrostructure of the cross-section in Fig. 8a shows only a small crack in the root region. The microstructure of this area (Fig. 8b and Fig. 8c) consists of fine precipitates and cracking along grain boundaries. Grains are twinned. Formation of grey phase at grain boundary is detected Fig. 8d. In addition, creep cavities/voids at grain boundaries have taken place Fig. 8b. No hardening was observed; hardness being the same for cracked and uncracked regions of the weld Fig. 5c. Neither bulk carbon analysis nor magnetic susceptibility measurement indicated carburization. Ahead of the root crack, formation

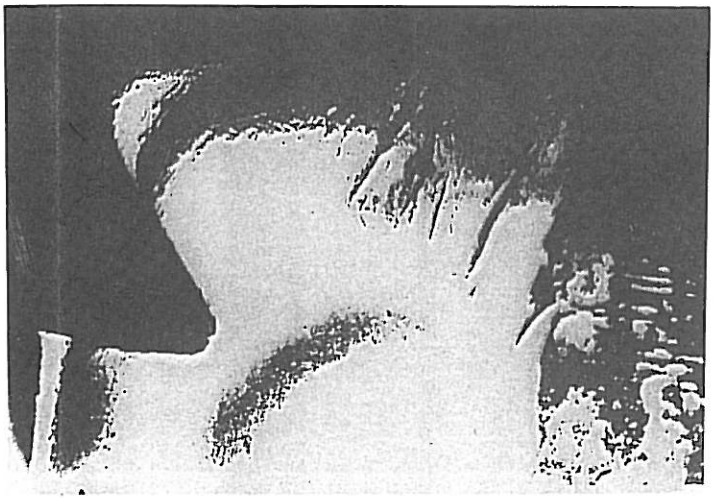


FIG. 6a. Sample I Microstructure of the cross section through thickness fracture region of the weld showing multiple internal cracks (etched).

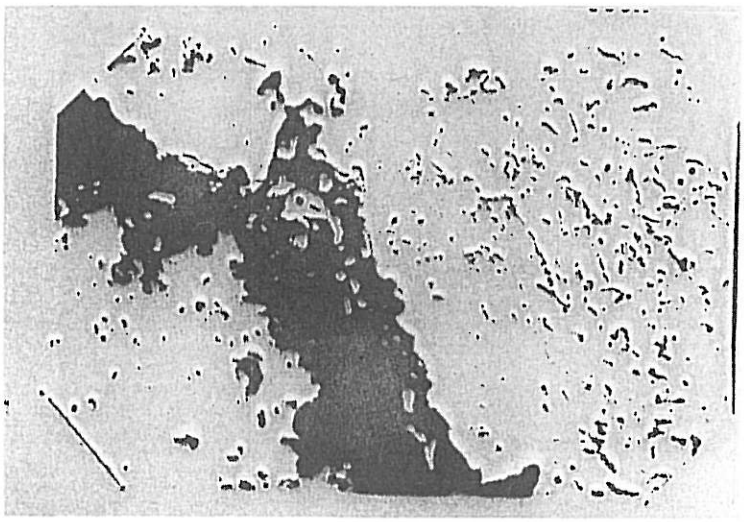


FIG. 6b. Root cracks associated with grey phase.

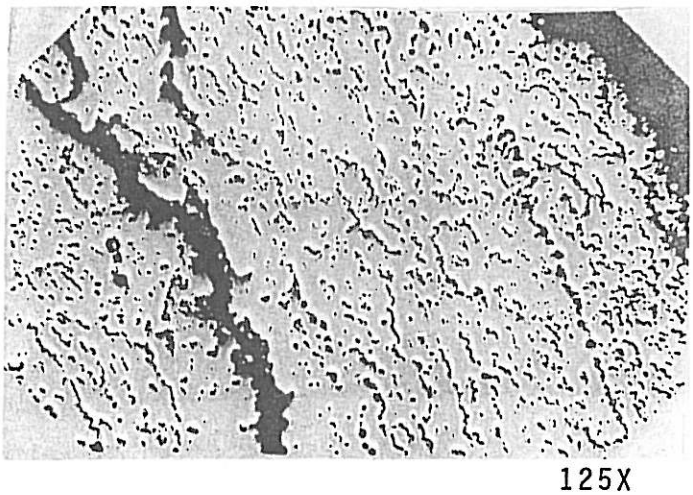
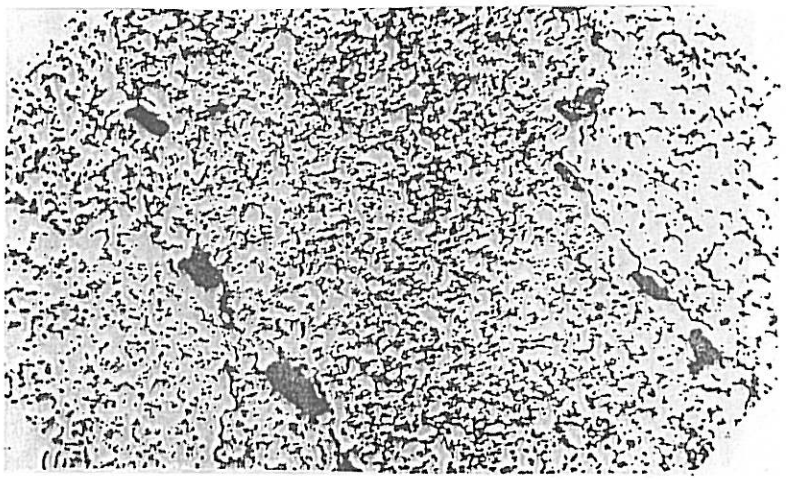
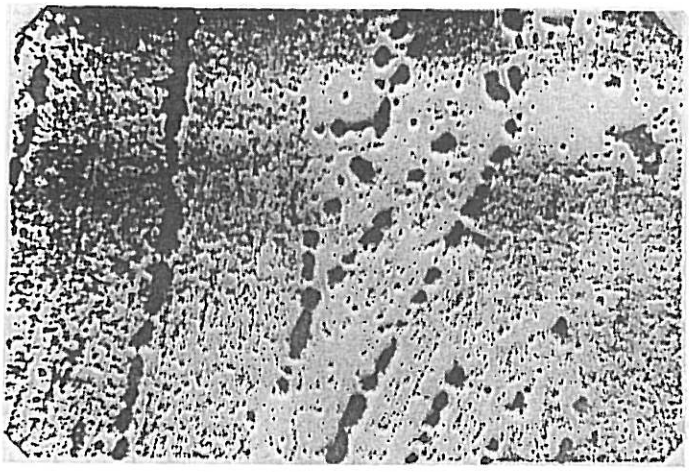


FIG. 6c. Root cracks and extensive precipitation along grain boundaries resulting from carburization of the root.



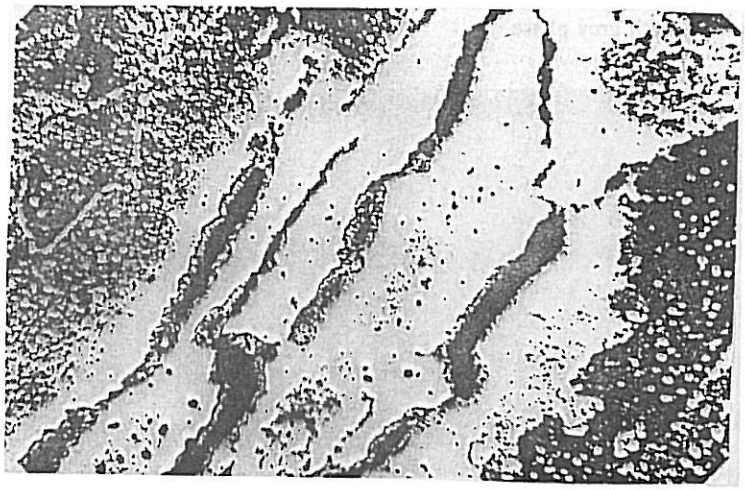
250 X

FIG. 6d. Continuous grain boundary precipitates (carbides) and different shaped precipitate, within grains.



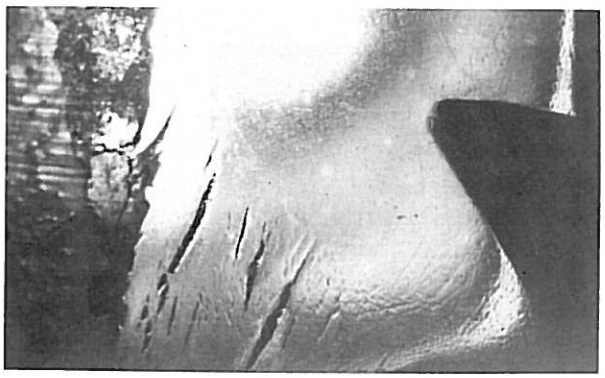
125 X

FIG. 6e. Away from fracture end, region showing fine precipitates and extensive, creep voids/cavities.



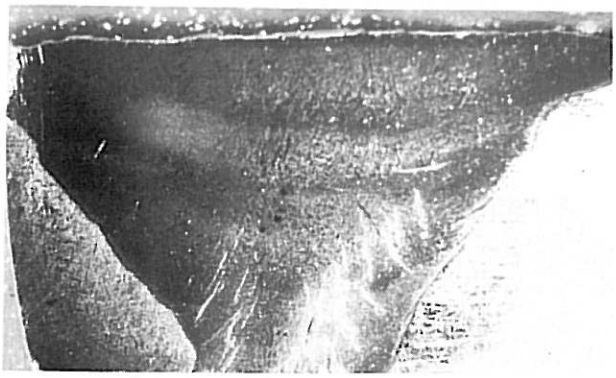
125 X

FIG. 6f. Grey phase fomation at grain boundaries and extraction through the grey phase.



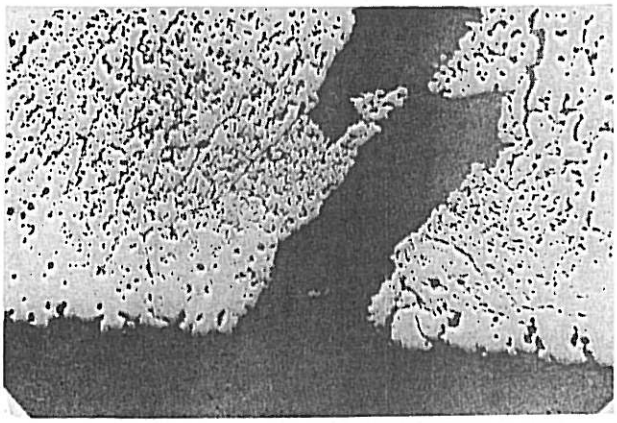
7 X

FIG. 7a. Sample V Macrostructure of the cross section showing multiple cracks in the root and away from WCL but no cracks formed in the outer weld surface (unetched).



7 X

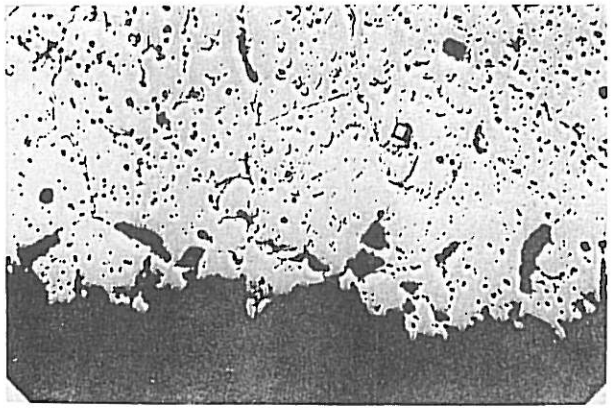
FIG. 7b. Same as Fig. 8(a) but after etching showing columnar grain structure of the weld metal.



125X

FIG. 7c. Cracking started from the root extensive precipitation within grains and at grain boundaries resulting from carburization (unetched).

of grey phase precipitates at grain boundaries was observed Fig. 8e. In the present case grey phase is essentially responsible for initiation of root crack and its partial propagation, Figs. 8d and Fig. 8e.



500X

FIG. 7d. Showing different shaped precipitates within grains and association of cavities with grain boundaries precipitates (unetched).

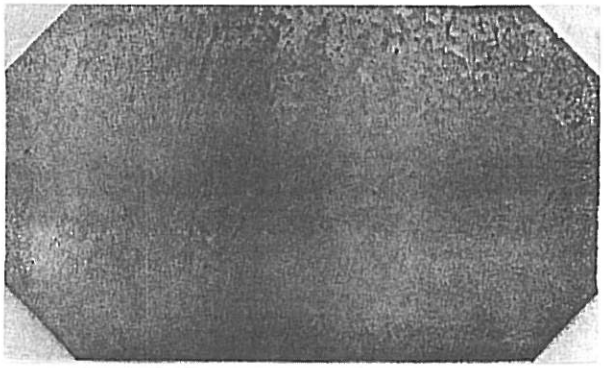
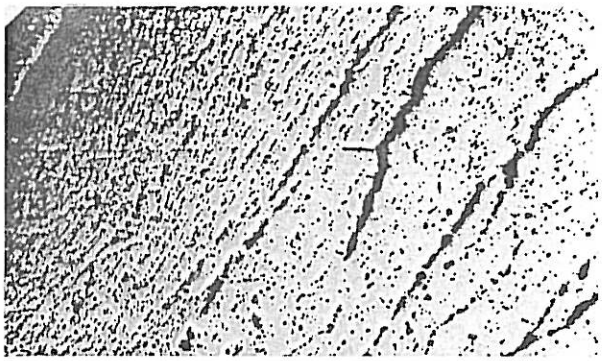


FIG. 7e. Middle of the weld showing finer precipitates and isolated creep cavities (unetched).



65X

FIG. 7f. Creep cracks and cavities adjacent to fusion line in the weld region away from the root region (etched).

E. EDAX

EDAX of grey phase at grain boundary (Fig. 9a) was observed to contain mainly Cr and Mn with some Ti as seen in Fig. 8b. EDAX shows absence of sulphur in the grey phase.

Figure 9c shows EDAX of grey phase at grain boundary revealing the grey phase to consist of only Mn and absence of Cr and Ti. Figure 9d shows

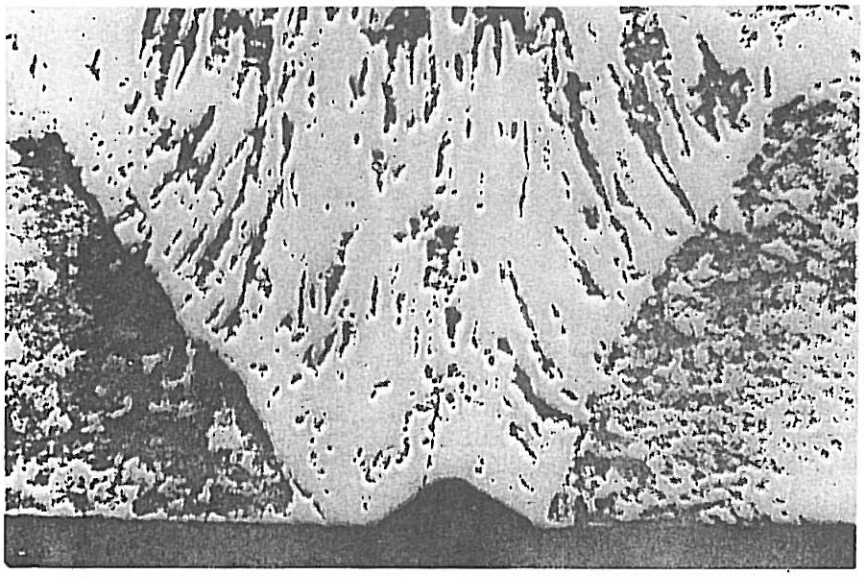


FIG. 8a. Macrostructure of the cross section of the weld region showing a root crack and columnar grain structure materials drilled from root bottom, (etched).

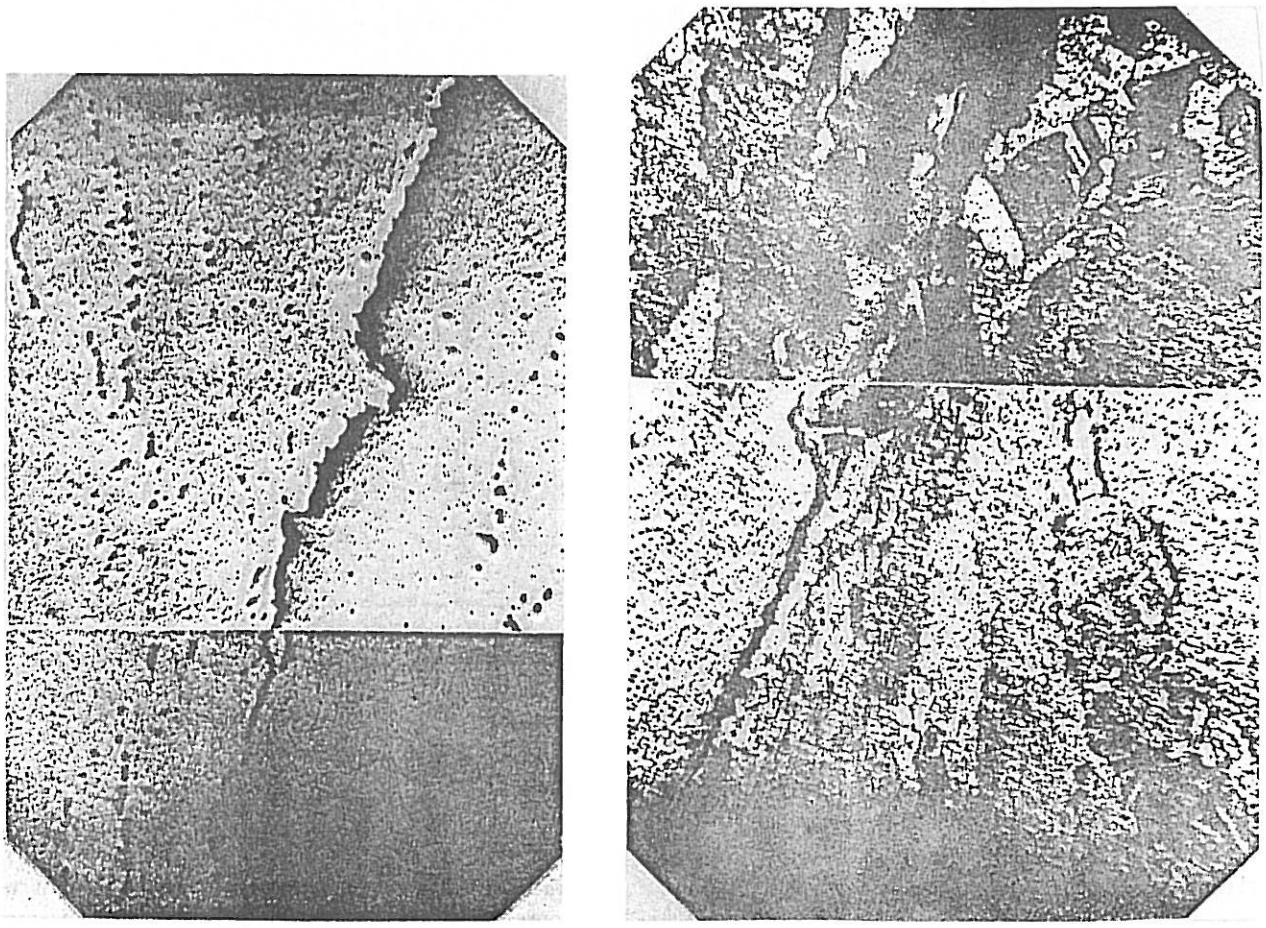


FIG. 8b,c. Root crack formation and its propagation in the root region not affected by carburization but affected by creep damage as seen around the crack and ahead of the crack.

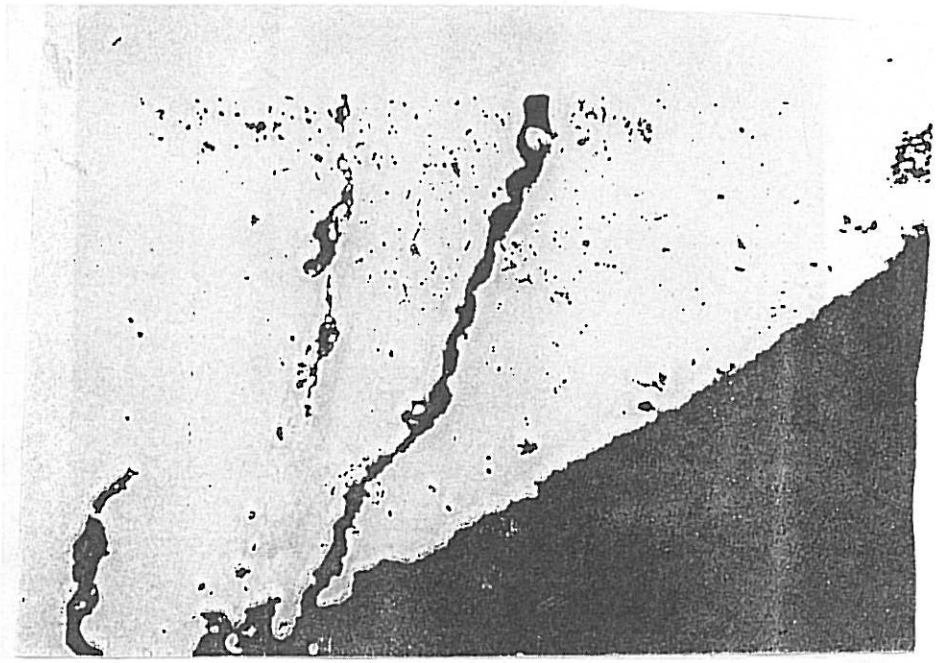


FIG. 8d. Grey phase formed at grain boundaries assisted nucleation of root crack.

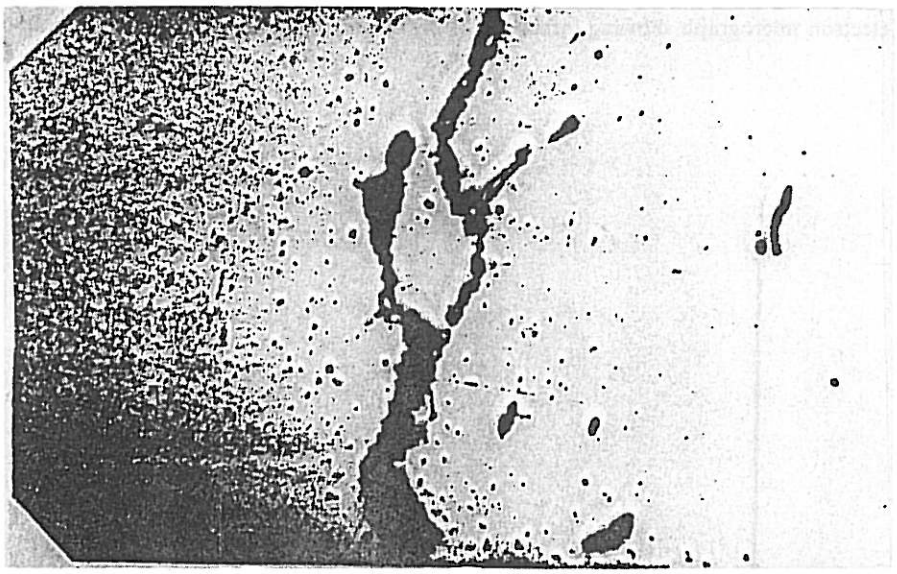


FIG. 8e. Grey phase facilitating crack propagation.

scanning electron micrograph, EDAX and quantitative chemical analysis of grey phase.

EDAX of rod shape precipitates in the matrix is shown in Fig. 9e, which reveals that this precipitates consist of Ni, Cr, Fe and Mn, major component being Ni and Cr.

CHEMICAL COMPOSITION

In view of the failure of the weld, chemical composition determined was only for the weld using atomic absorption spectrometer. Results are given in Table 2a. Composition for welding electrode used is listed in Table 2b. Analysis of Mo, Ti and Nb was not carried out for the weld.

Iron present in Weld Metal (WM) is higher while Ni is lower as compared with that in welding electrode. This difference results from dilution of welding driller metal caused by the admixture of the base metal. Base metals in the present case are dissimilar materials, Manurite 36X and Incoloy 800H being iron based alloys. Their composition are listed in Table 2b for reference.

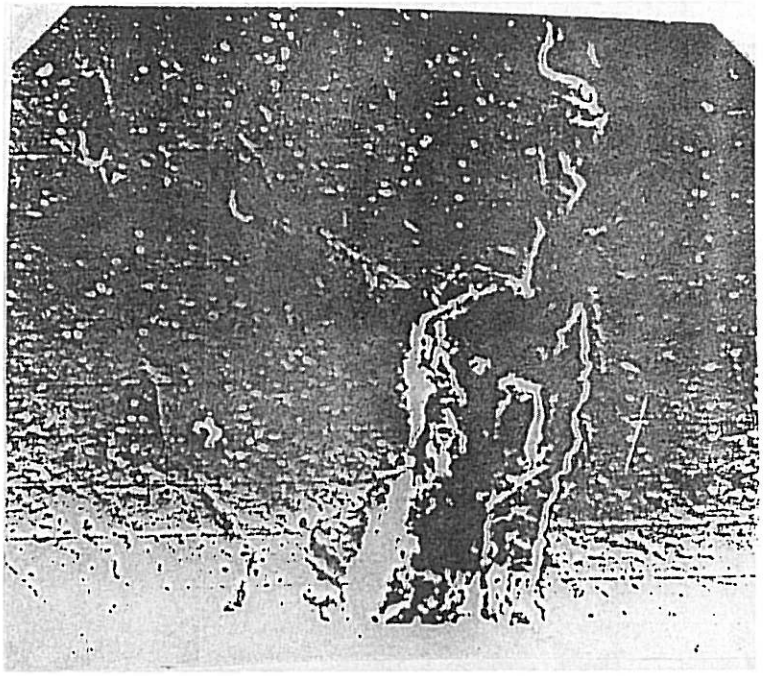


FIG. 9a. Scanning electron micrograph showing formation of brittle and porous grey phase at grain boundaries and matrix precipitates.

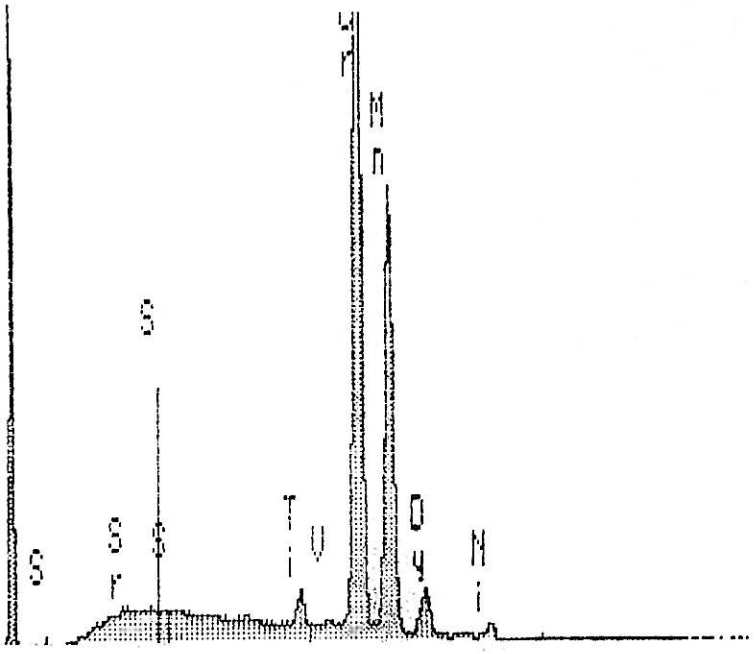


FIG. 9b. EDAX of grey phase precipitates showing presence of Cr, Mn and some Ti.

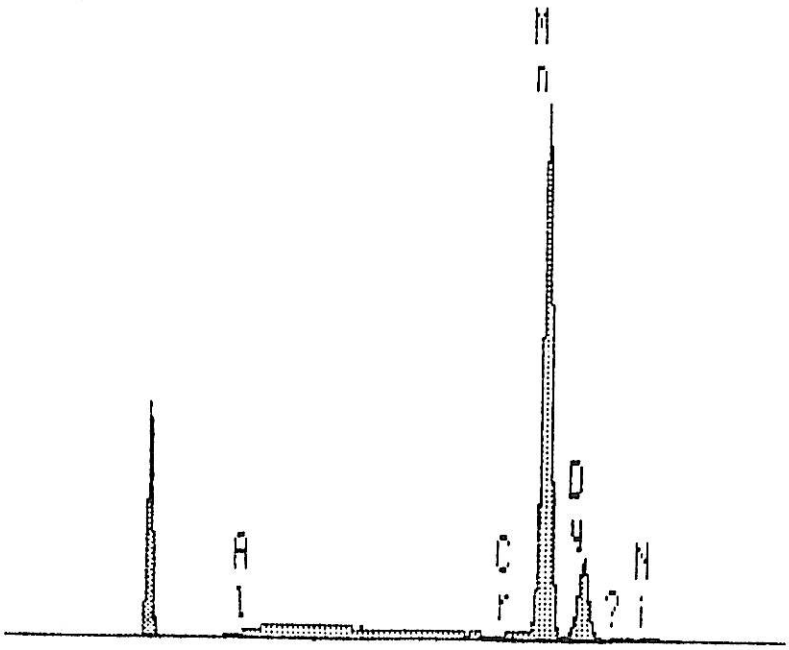
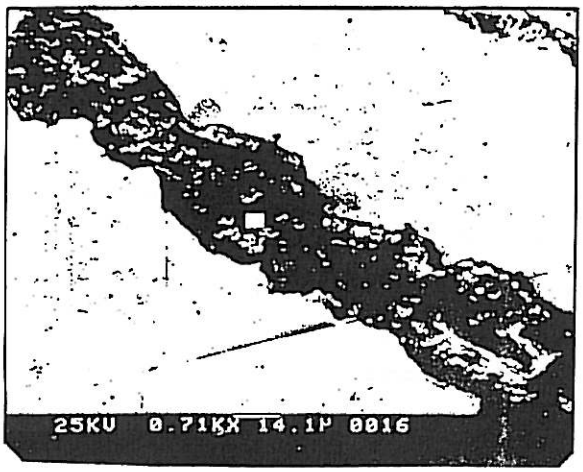


FIG. 9c. EDAX of grey phase facilitating crack propagation.



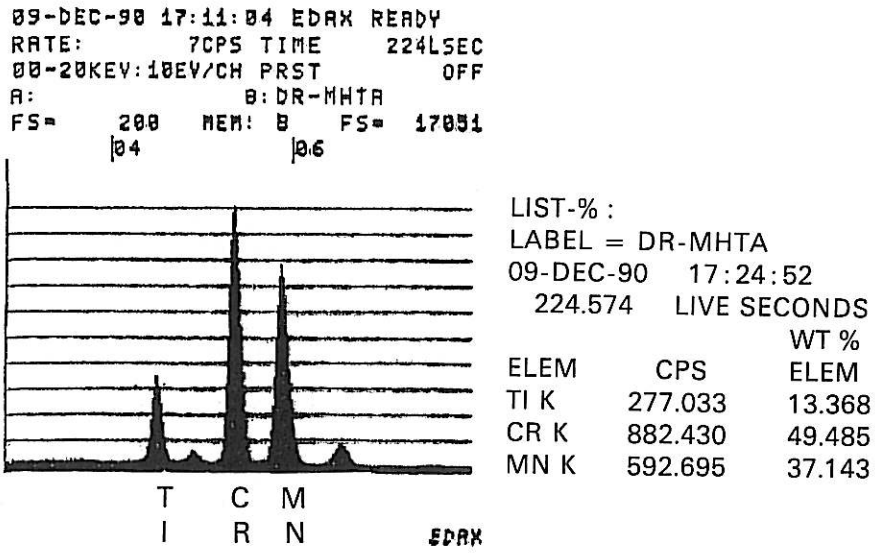


FIG. 9d. EDAX of the area marked in scanning electron micrograph and quantitative elemental composition of the grey phase.

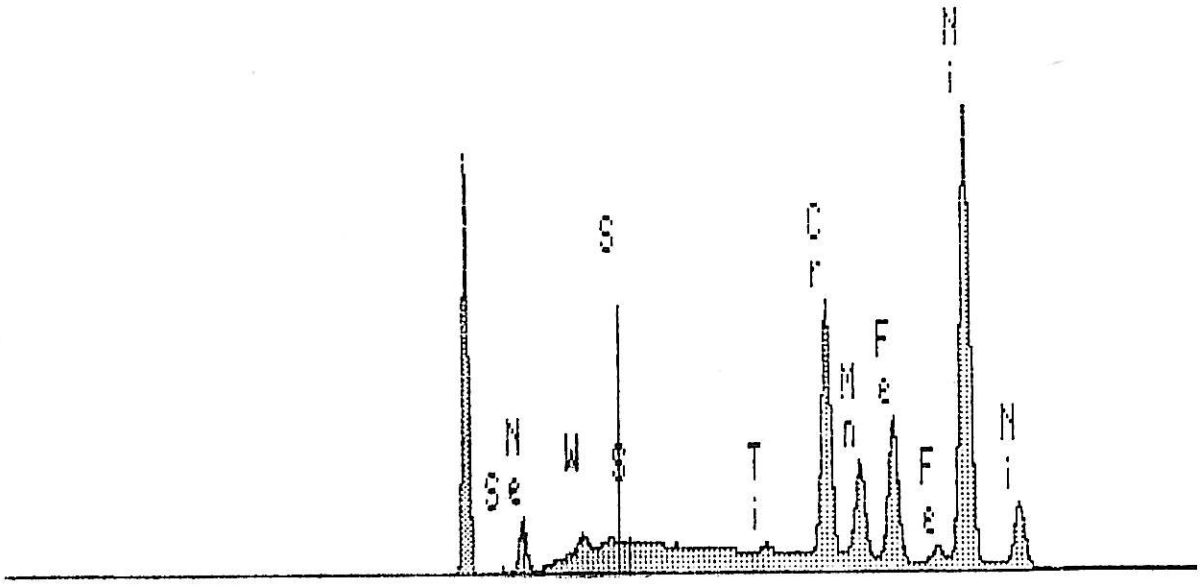


FIG. 9e. EDAX of the shape precipitates within the grain showing presence of Ni, Cr, Fe and Mn.

Table 2a. Chemical Composition of Welding Electrode ER. Ni-Cr-Fe_3

Element	C	Ni	Mn	Cr	Mo	Ti	Fe
%	0.05	67	5	19	1	2	3

Chemical Composition of Weld Metal

Element	Ni	Al	Cr	Fe	Mn
%	60	0.08	18.9	11.3	6.7

Table 2b. Manurite 36X

Element	C	Ni	Fe	Cr	Mn	Si	Nb	Ti
%	0.45	32–35	Balance	23–27	2	2	1	—

Incoloy 800H

Element	C	Ni	Fe	Cr	Mn	Si	Nb	Ti
%	0.08	32	45	21	—	—	—	0.04

DISCUSSION

Results of the present investigation establish that the weld suffered from localized carburization in some regions, creep voids/cracks and formation of brittle grey phase at grain boundaries. Evidence for localized carburization are magnetic susceptibility hardness and microstructural changes.

Formation of brittle grey phase at grain boundaries was detected in all the samples examined. However, it was detected in greater amount in weld regions cracked through thickness. This phase was brittle and provided sites for easy crack nucleation and propagation.

The weld metal is nickel base alloy and its chemical composition is given in Table 2a. Decker and Sims [1] have discussed metallurgy of nickle-base alloys. Its matrix structure is FCC austenite and the major second phases normally present are precipitates and carbides. FCC austenite, is a solid solution and among the alloying elements present Cr, Fe and Mo form solid solution, while Cr, Mo and Ti form carbides. The major precipitates phase is gamma prime (γ) in nickel alloys Ni, Al, Ti and Nb.

Microstructural changes observed such as carbides formation within grains and at grain boundaries, particularly in the cracked region of the weld, are due to localized carburization. Segregation of alloying elements at the grain boundaries led to the formation of brittle grey phase.

However, the types of carbides formed need to be identified. Not all the second phase precipitates are carbides. EDAX analysis of rod type precipitates seen in SEM was found to consist of Ni, Cr, Fe and the nature of this phase remains to be identified.

X-ray diffraction ad transmission electron microscopic studies are required to identify second phase precipitates formed.

Localized carburization, grey phase formation at grain boundaries and creep are the factors which emerge from the present study as the causes for the weld failure. Their role in the failure is considered. The partially cracked regions, as illustrated in Figs. 7a, 8a indicated that crack initiation started from the

root of the weld caused by localized carburization and formation of brittle grey phase at grain boundaries. However, crack propagation was caused by the accelerated creep due to increase stresses of the weld with the progress of fracture in the weld as in Fig. 4. The region of the weld where there had been hardly any carburization suffered from creep damage in the form of microcreep cracks/voids induced by higher stresses resulting from decreasing load bearing area. It may be stated that the extent of creep damage observed would have not taken place if stresses have not increased. In this region initiation of root crack and its partial propagation is attributed to the brittle grey phase at grain boundaries Fig. 4.

The region of the weld where there had been hardly any carburization suffered from creep damage in the form of microcreep cracks/voids induced by higher stresses resulting from decreasing load bearing area.

CONCLUSION

- Localized carburization, brittle grey phase formation at grain boundaries and creep are the factors responsible for the weld failure.
- The factors responsible for the fracture initiated from the root of the weld are the localized carburization of the root and formation of brittle grey phase at grain boundaries.
- Propagation of fracture, once initiated in the root of the weld, was assisted by creep and brittle grey phase formation at grain boundaries.

ACKNOWLEDGEMENT

The authors would like to thank the management of the Petroleum Research Centre for their encouragement to present this work and to Ras Lanuf Petrochemical Complex staff for their permission to carry out this work at the Petroleum Research Centre.

REFERENCES

[1] R.F. Decker and C.T. Sims, The Superalloys, (John Wiley and Sons, Inc., 1972), p. 33.
[2] M.W. Mucek, Materials Performance, 1983, vol. 23, No. 9, p. 25.